



Special Issue:

Recent Trends in Applied and Computational Mathematics

Proceedings of the Third International Conference on Recent Trends in Applied and Computational Mathematics (ICRTACM-2022)

School of Applied Sciences, Department of Mathematics,
Reva University, Bengaluru, India, 10th & 11th October, 2022

Editors: M. Vishu Kumar, A. Salma, B. N. Hanumagowda and U. Vijaya Chandra Kumar

Research Article

Effect of Micropolar Fluid Flow on Unsteady Convective Diffusive Mass Transfer in Doubly Connected Region

Indira Ramarao¹ , S. Jagadeesha*¹ , K. R. Rashmi¹  and K. R. Sreegowrav² 

¹Department of Mathematics, Nitte Meenakshi Institute of Technology, Bengaluru, India

²Department of Mathematics, School of Applied Science, REVA University, Bengaluru, India

*Corresponding author: jagadeeshas31@gmail.com

Received: March 4, 2023

Accepted: June 16, 2023

Abstract. Solute transfer in a micropolar fluid flowing between two concentric cylindrical tubes is considered. The governing equations are solved analytically for velocity. The species transport equation is solved by using a long-time approach following Sankara Subramanian and Gill model to obtain mean concentration and coefficients of dispersion. The results are analysed with respect to a catheterized artery for the parameter values available in the literature. The effects of micro-rotation, reaction rate, and inner tube radius on the diffusive, convective, and dispersion coefficients are analysed by graphically depicting the numerical results.

Keywords. Micropolar fluid, Dispersion, Catheterized artery, Species transport equation, Concentric cylinders

Mathematics Subject Classification (2020). 76Rxx

1. Introduction

Dispersion of solute or tracer particles has been a means to transfer in different flow regimes since Taylor [16]. A drug or a dye injected in a flow gets transported by means of dispersion, which includes convection and diffusion as well. Aris [1] also has developed models for pulsatile flows. Later a generalized model was developed large time by Sankarasubramanian and Gill [12]. Interphase mass transfer for large time was included by Sankarasubramanian and Gill [13]. A catalytic irreversible reaction of first order was assumed at the wall. Wall absorption was included for studying dispersion by Jiang and Chen [4].

Drug induced in the blood flow is transported through dispersion and studying wall absorption becomes very important. In this view many studies have been conducted. The catheter based drug delivery needs to understand dispersion in an annular region. Sankarasubramanian and Gill [13], Rao and Deshikachar [11] have developed theoretical model to describe the above said process and they have analysed that axial dispersion decreases with increase in inner radius. Axial mass transport by an asymptotic analysis was studied by Pedley and Kamm [8] by considering annular region. Numerical solution was obtained. A steady annular flow with reference to catheterized artery was considered, and dispersion of solute with chemical reaction at boundary was modelled by Sarkar and Jayaraman [14].

A catheterized artery creates an annular region in which catheter can be used to induce solute particles and blood flow could be Newtonian or non-Newtonian. In this regard Sarkar and Jayaraman [15] have studied generalized dispersion in concentric annular region with effects of absorption coefficient at the wall. Many authors have studied wall reaction at the wall using Newtonian or non-Newtonian flow (Nagarani *et al.* [7], Ramana and Sarojamma [9], Rana and Murthy [10]). Debnath *et al.* [2] assumed a three layered fluid flow and studied wall absorption. Multiphase flow is studied by Tiwari and Deo [17].

Umadevi *et al.* [18] have studied effect of particle drug considering two phase flow for blood in concentric annular region. Madhura *et al.* [5] have studied mass transfer in a doubly connected region by assuming annular region between eccentric cylinders. Venkataswamy *et al.* [19] have studied effect of viscoelastic flow by considering Jeffrey fluid with magnetic effect and analyzed mass transfer. Recently an analysis of stokes flow is conducted by Mourya *et al.* [6] assuming micropolar fluid.

In the present studies non-Newtonian nature of the blood flow is considered and modelled as a micropolar fluid. The effect of micro-rotation of suspended particles is studied. The generalized dispersion model of Sankarasubramanian and Gill [13] has been adopted for the current situation and analytical solution for mean concentration and the coefficients arising out of mass transfer at large time is calculated.

2. Mathematical Formulation

The blood vessel is modelled as a long cylindrical tube in which a catheter is inserted creating a concentric annular region as shown in the physical configuration.

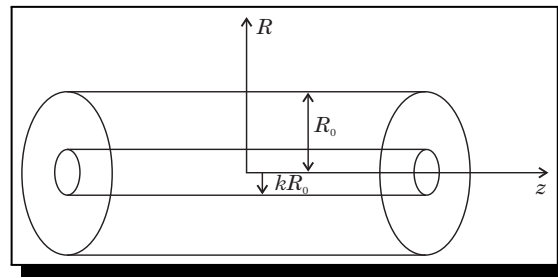


Figure 1. Physical configuration

The flow is assumed between the cylinders. The radius of outer cylinder is assumed to be and as the reference length. Flow is assumed to fully developed and steady, under these conditions the governing equations for a micropolar fluid are given by (Hayat and Ali [3]),

$$\nabla \cdot \vec{v} = 0, \tag{2.1}$$

$$\rho[\vec{v} \cdot \nabla \vec{v}] = -\nabla p + k(\nabla \times \vec{q}) - (\mu + k) \nabla^2 \vec{q}, \tag{2.2}$$

$$\rho j'[\vec{v} \cdot \nabla \vec{q}] = -2k\vec{q} + k(\nabla \times \vec{v}) - \gamma(\nabla \times \nabla \times \vec{q}) + (\alpha + \beta + \gamma)[\nabla(\nabla \cdot \vec{q})], \tag{2.3}$$

where \vec{v} and \vec{q} are velocity and micro-rotation vectors and $\mu, k, \alpha, \beta, \gamma$ are material constants.

For a fully developed flow, the above equations after non-dimensionalisation with the following quantities $r^* = \frac{r}{R_0}, w^* = \frac{w}{u_0}, u^* = \frac{u}{u_0}$ are given by

$$\frac{\partial u}{\partial r} + \frac{u}{r} + \frac{\partial w}{\partial z} = 0, \tag{2.4}$$

$$N \left\{ \frac{\partial w}{\partial r} + \frac{w}{r} \right\} + \frac{\partial^2 u}{\partial r^2} + \frac{1}{r} \frac{\partial u}{\partial r} = (1 - N) \frac{\partial p}{\partial z}, \tag{2.5}$$

$$2\vec{q} + \frac{\partial u}{\partial r} - \left(\frac{1 - N}{m^2} \right) \frac{\partial}{\partial r} \left[\frac{w}{r} + \frac{\partial w}{\partial r} \right] = 0, \tag{2.6}$$

where $\frac{\partial p}{\partial z}$ is the pressure gradient, $N = \frac{k}{\mu + k}$ and $m^2 = \frac{R_0^2 k(2\mu + k)}{\gamma^2(\mu + k)}$.

Solving the above equations analytically assuming no-slip condition at the boundary given by

$$w = 0, u = 0 \text{ on } r = k \text{ and } r = 1. \tag{2.7}$$

The exact solution is given by

$$w = Ay_1(r) + By_2(r) + Cy_3(r) + aP, \tag{2.8}$$

$$u = \left(\frac{2 - N}{m^2} \right) [A\phi_1(r) + B\phi_2(r) + C\phi_3(r)] - aP \left[2r + \frac{1}{r} \left(\frac{2 - N}{m^2} \right) \right] + P. \tag{2.9}$$

The constants are listed in Appendix.

3. Mathematical Model for Dispersion

The species transport equation in non-dimensional form is given by

$$\frac{\partial c}{\partial t} + w \frac{\partial c}{\partial z} = \frac{1}{r} \frac{\partial}{\partial r} \left(r \frac{\partial c}{\partial r} \right) + \frac{1}{Pe^2} \frac{\partial^2 c}{\partial z^2}, \tag{3.1}$$

where Pe is the Peclet number.

The trace is induced in the flow. Initial and boundary conditions are given by

$$C(0, r, z) = \beta_2(z)\beta_1(r), \tag{3.2}$$

where $\beta_2(z) = \frac{\delta(z)}{PeR_0^2}$, $\delta(z)$ is the Dirac delta function and $\beta_1(r) = \begin{cases} 1, & k < r \leq a, \\ 0, & a < r \leq 1. \end{cases}$

Boundary conditions at the catheter wall and arterial wall are as follows:

$$\frac{\partial c}{\partial r} = 0 \quad \text{on } r = k, \tag{3.3}$$

$$\frac{\partial c}{\partial r} = -\beta c \quad \text{on } r = 1. \tag{3.4}$$

Following Jiang and Chen [4], the concentration can be assumed in the following series form:

$$C(r, t, z) = \sum f_n(t, r) \frac{\partial^n c_m}{\partial z^n}, \tag{3.5}$$

where $c_m = \frac{\int_0^{2\pi} \int_k^1 cr dr d\theta}{\int_0^{2\pi} \int_k^1 cr dr d\theta} = \frac{2}{1-k^2} \int_k^1 cr dr$.

Here f_n can be determined from the equation (3.1), substituting the equation (3.2) to equation (3.4).

Mean concentration can be obtained by truncating equation (3.5) in the form,

$$\frac{\partial c_m}{\partial t} = M_0(t)c_m + M_1(t)\frac{\partial c_m}{\partial z} + M_2(t)\frac{\partial^2 c_m}{\partial z^2}. \tag{3.6}$$

In the above model $M_0(t)$ is called the exchange parameter and arises due to first order equation at the wall. $M_1(t)$ is the convective coefficient on which the coefficient which is inclusive of convection, diffusion and exchange. Substitution of equation (3.5) in equation (3.1) and making use of equation (3.6), equating coefficients of $\frac{\partial c_m}{\partial t}$, $n = 0, 1, 2, 3, \dots$ following equations are generated:

$$\frac{\partial f_n}{\partial t} - \frac{\partial^2 f_n}{\partial r^2} - \frac{1}{r} \frac{\partial f_n}{\partial r} + w(r)f_{n-1} - \frac{1}{Pe^2}f_{n-2} + \sum_{i=0}^n f_{n-i}M_i = 0, \quad n = 0, 1, 2, 3, \dots, \tag{3.7}$$

with $f_{-1} = 0 = f_{-2}$.

We can find M_n as,

$$M_n(t) = \frac{2}{1-k^2} \left\{ \frac{\partial}{\partial r} [f_n(\tau, 1)] - \int_k^1 rw(r)f_n(t, r)dr \right\} + \frac{\delta_{n,2}}{Pe^2}, \quad n = 0, 1, 2, 3, \dots, \tag{3.8}$$

where $\delta_{n,2} = \begin{cases} 1, & n = 2, \\ 0, & \text{otherwise.} \end{cases}$ The initial and boundary conditions reduces to,

$$c_m(0, z) = \frac{2}{1-k^2} \int_k^1 rB_1(r)dr, \tag{3.9}$$

$$C(0, r, z) = f_0(0, z)c_m(0, z), \tag{3.10}$$

$$f_0(0, r) = \frac{1-k^2}{2} \left(\frac{B_1(r)}{\int_k^1 rB_1(r)dr} \right), \tag{3.11}$$

$$\int_k^1 rf_n(t, r)dr = \delta_{n,0} \left(\frac{1-k^2}{2} \right), \tag{3.12}$$

$$\frac{\partial f_i}{\partial r}(t, 1) = -\beta f_i(\tau, 1), \quad \frac{\partial f_i}{\partial r}(t, r) = 0, \quad i = 0, 1, 2. \tag{3.13}$$

Using the transformation,

$$f_0(t, r) = g_0(t, r)e^{-\int_0^t M_0(\eta)d\eta}, \tag{3.14}$$

and solving the resulting equation,

$$\frac{\partial g_0}{\partial t} = \frac{\partial^2 g_0}{\partial r^2} + \frac{1}{r} \frac{\partial g_0}{\partial r} \tag{3.15}$$

subject to

$$g_0(0, r) = \frac{1 - k^2}{2} \left(\frac{B_1(r)}{\int_k^1 B_1(r)dr} \right), \tag{3.16}$$

$$\left. \begin{aligned} \frac{\partial g_0}{\partial r} &= -\beta g_0 \text{ on } r = 1, \\ \frac{\partial g_0}{\partial r} &= 0 \text{ on } r = k. \end{aligned} \right\} \tag{3.17}$$

The solution is obtained as,

$$g_0 = \sum \frac{A_n}{f_1(\mu_n k)} E_n(\mu_n r) e^{-\mu_n^2 \tau}, \tag{3.18}$$

where

$$A_n = \frac{\mu_n^2(1 - k^2)f_1(\mu_n k) \int_k^1 r B_1(r) E_n(\mu_n r) dr}{[(\mu_n^2 + \beta^2)E_n^2(\mu_n) - k^2 \mu_n^2 E_n^2(\mu_n k)] \int_k^1 r B_1(r) dr}$$

and

$$E_n(\mu_n r) = Y_0(\mu_n r)J_1(\mu_n k) - Y_1(\mu_n k)J_0(\mu_n r).$$

Here μ_n are the Eigen values satisfying the condition,

$$\mu_n [Y_1(\mu_n k)J_1(\mu_n) - Y_1(\mu_n)J_1(\mu_n k)] + \beta [Y_0(\mu_n)J_1(\mu_n k) - Y_1(\mu_n k)J_0(\mu_n)] = 0. \tag{3.19}$$

Using the equations (3.14) and (3.16), the exchange coefficient is obtained in the form,

$$M_0(\tau) = \frac{-\sum_{n=0}^{\infty} \frac{A_n}{J_1(\mu_n k)} \mu_n [Y_1(\mu_n)J_1(\mu_n k) - Y_1(\mu_n k)J_1(\mu_n)] e^{-\mu_n^2 t}}{\sum_{n=0}^{\infty} \frac{A_n}{J_1(\mu_n k)} [Y_1(\mu_n)J_1(\mu_n k) - Y_1(\mu_n k)J_1(\mu_n)] e^{-\mu_n^2 t}}. \tag{3.20}$$

The equations pertaining to f_1 and f_2 are complicated, hence the computation is affected only for large time analysis. Hence as $t \rightarrow \infty$, the above equations for f_0 and M_0 reduces to:

$$f_0(\infty, r) = \frac{(1 - k^2) \mu_0 [Y_0(\mu_0 r)J_1(\mu_0 k) - Y_1(\mu_0 k)J_0(\mu_0 r)]}{2 \{Y_1(\mu_0)J_1(\mu_0 k) - Y_1(\mu_0 k)J_1(\mu_0)\}}, \tag{3.21}$$

where $\mu_0(\infty) = -\mu_0^2$.

For large time analysis, the equation (3.7) reduces to

$$\frac{\partial^2 f_1}{\partial r^2} + \frac{1}{r} \frac{\partial f_1}{\partial r} + \mu_0 f_1 = w(r)f_0 + M_1 f_0, \tag{3.22}$$

$$\frac{\partial^2 f_2}{\partial r^2} + \frac{1}{r} \frac{\partial f_2}{\partial r} - w(r)f_1 + \frac{1}{Pe^2} f_0 + \sum_{i=0}^2 f_{2-i} M_i \tag{3.23}$$

subject to

$$\left. \begin{aligned} \frac{\partial f_i}{\partial r} &= -\beta f_i \text{ at } r = 1, \\ \frac{\partial f_i}{\partial r} &= 0 \text{ at } r = k. \end{aligned} \right\} \tag{3.24}$$

Solving these for large time $t \rightarrow \infty$, the coefficients are obtained by

$$M_1(\infty) = \frac{-4\mu_0[Y_1(\mu_0)J_1(\mu_0k) - Y_1(\mu_0k)J_1(\mu_0)] \int_k^1 r w(r) E_0(\mu_0 r) f_0(r) dr}{(1 - k^2)[(\mu_0^2 + \beta^2)\{E_0(\mu_0)\}^2 - k^2\mu_0^2\{E_0(\mu_0k)\}^2]}, \tag{3.25}$$

$$f_1(r) = \sum_{n=0}^{\infty} \frac{A_{1n} E_n(\mu_n r)}{J_1(\mu_n k)}, \tag{3.26}$$

where

$$A_{1n} = \begin{cases} \frac{\int_k^1 r \{w(r) + M_0\} f_0(r) E_n(\mu_n r) dr}{J_1(\mu_n k) (\mu_0^2 - \mu_n^2)}, & \text{for } n \geq 1, \\ -\frac{J_1(\mu_n k)}{\int_k^1 r f_0(r) E_0(\mu_0 r) dr} \sum_{n=1}^{\infty} \frac{A_{1n}}{J_1(\mu_n k)} \int_k^1 r E_n(\mu_n r) dr, & \text{for } n = 0, \end{cases}$$

$$M_2(\tau) = \frac{1}{Pe^2} - \frac{\int_k^1 r [w(r) + M_1] E_0(\mu_0 r) f_1(r) dr}{\int_k^1 r E_0(\mu_0 r) f_0(r) dr}. \tag{3.27}$$

Using the above expressions for M_0 , M_1 and M_2 in truncated equation for mean concentration where solution can be obtained as

$$c_m = \frac{1}{2Pe\sqrt{\pi T}} e^{\xi - \frac{\psi^2}{4T}}, \tag{3.28}$$

where

$$\xi(t) = \int_0^t M_0(\eta) d\eta,$$

$$\psi(t, z) = z + \int_0^t M_1(\eta) d\eta,$$

$$T(t) = \int_0^t M_2(\eta) d\eta,$$

and for large time,

$$\xi(t) \rightarrow M_0(\infty)t,$$

$$\psi(t, z) \rightarrow z + M_1(\infty)t,$$

$$T(t) \rightarrow M_2(\infty)t.$$

4. Results and Discussion

A catheterized artery is modeled as a concentric annular region bounded by cylindrical tubes of radius kR_0 and R_0 . There is a first order reaction present near artery wall and no slip condition is assumed for velocity on both tubes. The solution obtained is numerically evaluated. The Eigen values μ_n for $n = 0, 1, 2, 3, \dots$ are evaluated numerically by adopting Newton-Raphson method. The coefficients of exchange, convection and dispersion are numerically evaluated and graphically depicted. The effect of micro rotation parameter m on these coefficients is analysed.

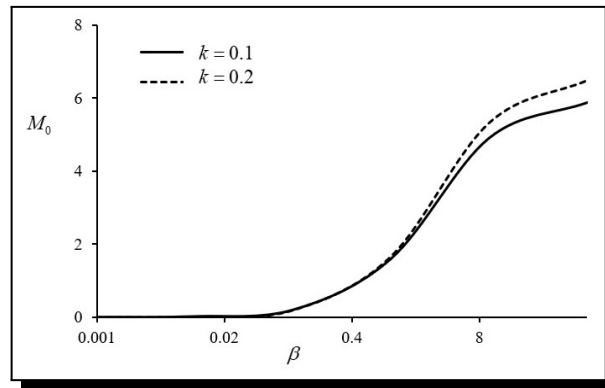


Figure 2. Plot of absorption coefficient against flux at the wall

The exchange coefficient is affected only due to reaction at wall and varies with absorption parameter. Figure 2 shows variation of exchange coefficient M_0 with absorption parameter β for large time. The curve shows increasing behaviour and attains a constant value as $\beta \rightarrow \infty$. The coefficient $M_0(\tau)$, due to flux present at the wall of the tube. M_0 will be negative on the account of mass depletion across the wall. At large time, M_0 and μ_0^2 depends on β alone. Figure 2 shows, absorption coefficient plotted against flux parameter β and different values of inner tube radius k . As β increases, the absorption coefficient increases.

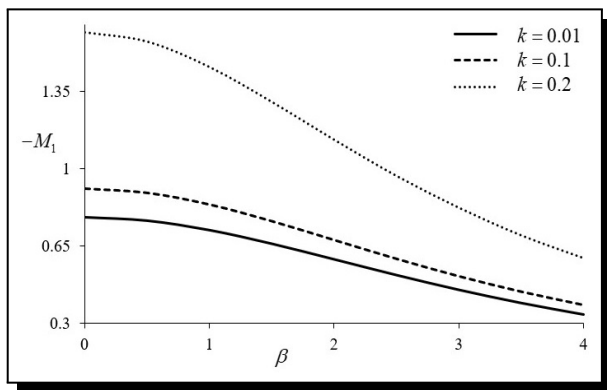


Figure 3. Convection coefficient vs flux parameter for different inner tube radius

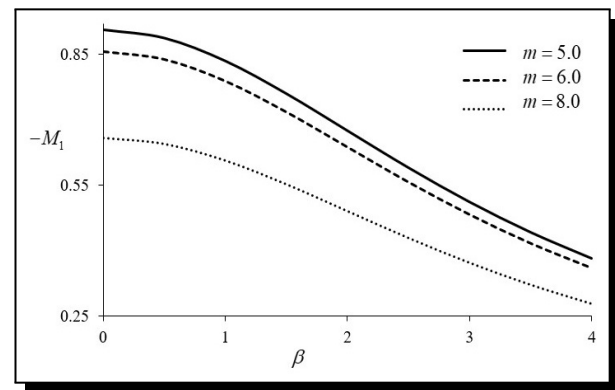


Figure 4. Concentration coefficient vs flux parameter for different micro-rotation parameter

The negative convective coefficient decreases with increasing β and increases with increasing inner radius k . The solute is convected across the tube and depends on velocity. At $\beta = 0$, the convection happens with average velocity and later gets influenced by the flux at wall. Increase in inner tube radius is to increase convective coefficient as the velocity increase in order to maintain constant volume flow rate. This is evident in Figure 3. Figure 4 describes the effect of micro-rotation parameter on the convective coefficient. As micro-rotation parameter increases, the convection coefficient decreases due to resistance created by micro-rotation of particles. Higher value of m indicates higher angular velocity to flow which reduce the solute being convected.

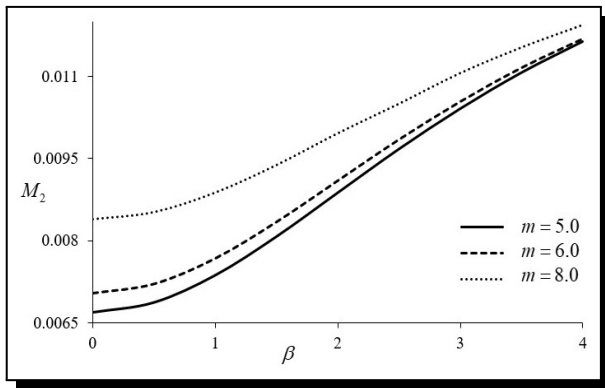


Figure 5. Dispersion coefficient vs flux parameter for different micro-rotation parameter

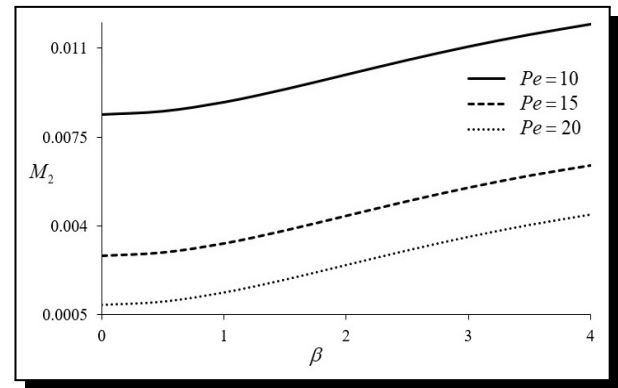


Figure 6. Dispersion coefficient vs flux parameter for different Peclet number

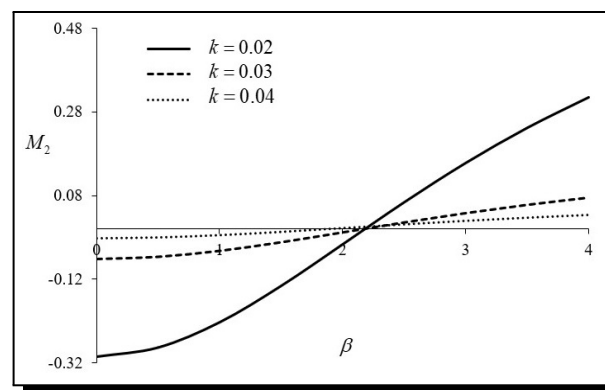


Figure 7. Dispersion coefficient vs flux parameter for different inner tube radius

Figure 5 depict the plot of dispersion coefficient which show combined effect of convection and diffusion against the flux coefficient β . Figure 5 shows the validation of micro-rotation. Figure 6 depicts effect of Peclet number and Figure 7 shows the effect of inner tube radius k . The dispersion coefficient increases exponentially in all cases. Effect of micro-rotation is to dispersion, hence as m increases, the dispersion increases. The micro-rotation augments diffusion but accelerates convection as a result of which with increase in m , increases dispersion coefficient.

Diffusion is inversely proportional to Peclet number. For a constant micro-rotation parameter, diffusion increases with decreasing Peclet number and hence increase in dispersion coefficient with decreasing Peclet number.

Increase in inner tube radius reduces area of cross section for the flow. Smaller radius dispersion coefficient increases exponentially with flux from a lower initial value to higher value. As k increases M_2 is higher for low flux value but the pattern changes for larger flux at the wall. The flux corresponds to diffusion towards the wall and as more solute moves towards the wall lower k value provides larger fluid space to diffuse towards the wall.

Figures 9 and 10 represent velocity profile along radial direction and Figures 11 and 12 represent average concentration as a function of long time.

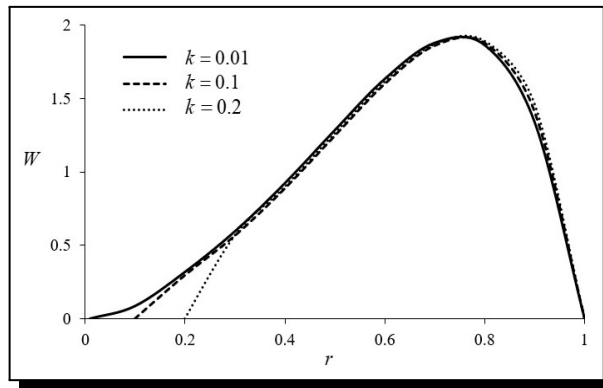


Figure 8. Radial velocity profile for different inner tube radius

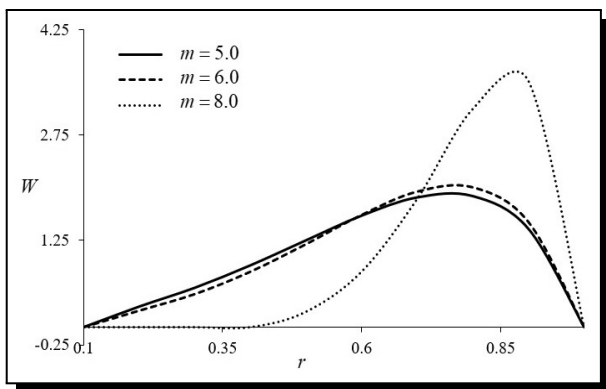


Figure 9. Radial velocity profile for different micro-rotation parameter

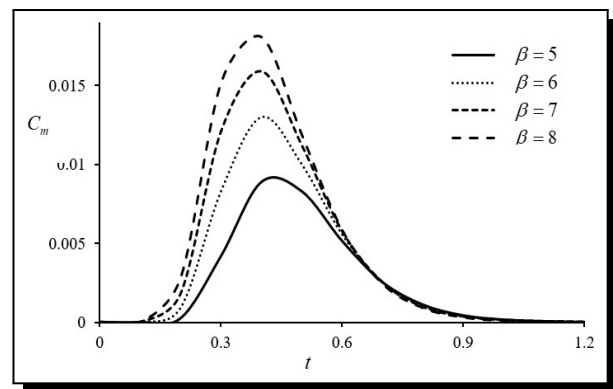


Figure 10. Average axial concentration profile for different values of flux at the wall

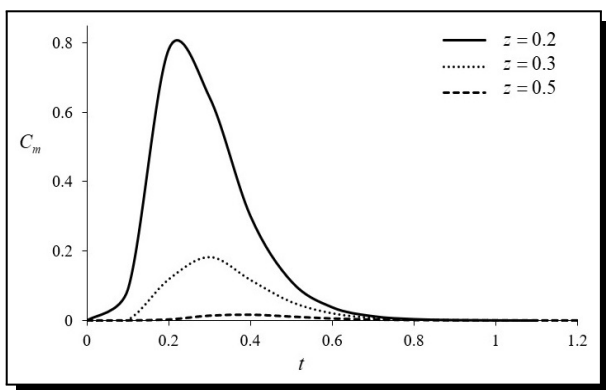


Figure 11. Average axial concentration profile for different axial position

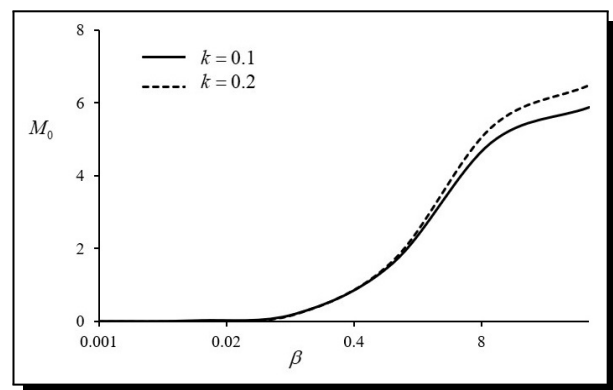


Figure 12. Average axial concentration profile for different microrotation parameter

The velocity profile deviates little bit from being parabolic and skewed towards the wall. Higher velocity is seen towards the wall as it is known that the particulate matter accumulate around the axis. Effect of inner tube radius is not predominant and observed only near the inner wall. The effect of micro-rotation parameter is more on velocity. As m increases from Figure 6 and 8, the velocity close to the inner wall remains zero and increase to a large value near the outer wall. As rotation is high, the impedance is seen near inner wall where micro-sized particles accumulate and more fluid will be present near outer wall.

Mean concentration is mainly affected by the flux near the wall and the peak in the curve shifts towards left as β increases. Peak for $\beta = 5$ is around 0.6 where as for $\beta = 8$ it is at $t = 0.5$. Initially concentration increases and around time $t = 1.0$, concentration reduces to almost zero. Figure 11 shows mean concentration for different axial positions. The concentration near the entrance shows very high value compared to mid of the tube in the axial direction. The depletion of concentration is seen along the axis due to convection. Figure 12 shows mean concentration for different micro-rotation parameter which shows increasing tendency with increase in m . This is due to accelerated convection in presence of micro-rotation.

5. Conclusions

The study highlights the effect of micro-rotation on the dispersion of solute particles in a micropolar fluid flowing in a concentric annular region. The method adopted is large-time analysis developed by Sankarasubramanian and Gill. The physical configuration considered is due to insertion of a catheter in an artery. Since rate of flow is based on requirement of surrounding tissue, area of cross-section decreases due to insertion, there will be an increase in the pressure gradient and hence velocity. These factors also have an effect on species transport. As the geometry and processes are complicated; exact solution is not possible. For the large time, average concentration is obtained by the series expansion technique. The three major coefficients of mass transfer and average axial concentration is analysed. M_0 is due to diffusion, and velocity does not affect it. M_1 is the convective coefficient, maximum effect of micro-rotation is on M_1 . As micro-rotation increases M_1 increases. M_2 is convective diffusion, called dispersion, which is also affected by micro-rotation. The velocity profile shows a shift towards the outer wall due to micro-rotation. The coefficients of mass transfer and average axial concentration are evaluated and plotted. M_0 is independent of flow and purely diffusive, M_1 and M_2 velocity dependent, M_1 being convective and M_2 being the combined effect of convection and diffusion. The effect of the inner tube radius is discussed. Convection increases as micro-rotation increases, and convective transfer becomes dominant. Micro-rotation shifts the flow towards the wall and is effective in transferring more solute towards the wall.

Acknowledgements

The authors extend their special thanks the management of Nitte Meenakshi Institute of Technology, Bengaluru and REVA University, Bengaluru for their cooperation in bringing out of this work.

Appendix

$$a = \frac{(1-N)m^2}{2-N},$$

$$y_1(r) = \sum \frac{m^{2k} r^{k+1}}{(k+2)!k!},$$

$$y_2(r) = \sum \frac{m^{2k} r^{k+1}}{(k+2)!k!} \{\log r + \psi_1(k)\},$$

$$\psi_1(k) = \sum_{i=2}^k -\frac{1}{i+2} - \sum_{i=0}^{k-2} \frac{1}{(i+2)^2},$$

$$y_3(r) = \sum \frac{m^{2k} r^{k+1}}{(k+2)!k!} \{(\log r)^2 + 2\psi(k)\log r + \psi_2(k)\},$$

$$\psi_2(k) = \sum_{i=2}^k \frac{1}{(i+2)^2} + \sum_{i=0}^{k-2} \frac{1}{(i+2)^2},$$

$$\phi_i(r) = \int \left(y_i'' + \frac{1}{r} y_i' - \frac{1}{r^2} y_i \right) dr, \quad \text{for } i = 1, 2, 3, \dots,$$

$$f_{1i} = \phi_i(1) - \phi_i(R_0),$$

$$f_1 = 2 \left(\frac{2-N}{m^2} \right) (1-R_0) + 1 - \frac{1}{R_0},$$

$$b_{22} = f_{12} y_1(k) - f_{11} y_2(k),$$

$$c_{33} = b_{23} b_{32} - b_{22} b_{33},$$

$$b_{23} = f_{13} y_1(k) - f_{11} y_3(k),$$

$$c_3 = b_1 b_{23} - b_2 b_{22},$$

$$b_1 = f_{11} y_1(k) - f_{11},$$

$$b_{32} = f_{12} y_1(1) - f_{11} y_2(1),$$

$$b_2 = f_{11} y_1(1) - f_{11},$$

$$b_{33} = f_{13} y_1(1) - f_{11} y_3(1),$$

$$A = \frac{f_1 - C f_{13} - B f_{12}}{f_{11}},$$

$$B = \frac{b_1 - b_{23} C}{b_{22}},$$

$$C = \frac{c_3}{c_{33}}.$$

Competing Interests

The authors declare that they have no competing interests.

Authors' Contributions

All the authors contributed significantly in writing this article. The authors read and approved the final manuscript.

References

- [1] R. Aris, On the dispersion of a solute in a fluid flowing through a tube, *Proceedings of the Royal Society of London A: Mathematical, Physical and Engineering Sciences* **235**(1200) (1956), 67 – 77, DOI: 10.1098/rspa.1956.0065.
- [2] S. Debnath, A. K. Saha, B. S. Mazumder and A. K. Roy, Dispersion phenomena of reactive solute in a pulsatile flow of three-layer liquids, *Physics of Fluids* **29** (2017), 097107, DOI: 10.1063/1.5001962.
- [3] T. Hayat and N. Ali, Effects of an endoscope on peristaltic flow of a micropolar fluid, *Mathematical and Computer Modelling* **48**(5-6) (2008), 721 – 733, DOI: 10.1016/j.mcm.2007.11.004.
- [4] W. Q. Jiang and G. Q. Chen, Solution of Gill's generalized dispersion model: Solute transport in Poiseuille flow with wall absorption, *International Journal of Heat and Mass Transfer* **127**(B) (2018), 34 – 43, DOI: 10.1016/j.ijheatmasstransfer.2018.07.003.
- [5] K. Madhura, R. Indira, S. P. Suma and S. Jagadeesha, An analytical study of mass transfer in doubly connected region, *Global Journal of Pure and Applied Mathematics* **14**(11) (2018), 1479 – 1487, URL: https://www.ripublication.com/gjpam18/gjpamv14n11_05.pdf.
- [6] D. K. Maurya, S. Deo and D. Y. Khanukaeva, Analysis of Stokes flow of micropolar fluid through a porous cylinder, *Mathematical Methods in the Applied Sciences* **44**(8) (2021), 6647 – 6665, DOI: 10.1002/mma.7214.
- [7] P. Nagarani, G. Sarojamma and G. Jayaraman, Effect of boundary absorption on dispersion in Casson fluid flow in an annulus: application to catheterized artery, *Acta Mechanica* **202** (2009), 47 – 63, DOI: 10.1007/s00707-008-0013-y.
- [8] T. J. Pedley and R. D. Kamm, The effect of secondary motion on axial transport in oscillatory tube flow, *Journal of Fluid Mechanics* **193** (1988), 347 – 367, DOI: 10.1017/S0022112088002174.
- [9] B. Ramana and G. Sarojamma, Unsteady convective diffusion in a Herschel-Bulkley fluid in a conduit with interphase mass transfer, *International Journal of Mathematical Modelling & Computations* **2**(3) (2012), 159 – 179, URL: https://ijm2c.ctb.iau.ir/article_521797.html.
- [10] J. Rana and P. V. S. N. Murthy, Unsteady solute dispersion in non-Newtonian fluid flow in a tube with wall absorption, *Proceedings of the Royal Society of London A: Mathematical, Physical and Engineering Sciences* **472**(193) (2016), 20160294, DOI: 10.1098/rspa.2016.0294.
- [11] A. R. Rao and K. S. Deshikachar, An exact analysis of unsteady convective diffusion in an annular pipe, *Journal of Applied Mathematics and Mechanics* **67**(3) (1987), 189 – 195, DOI: 10.1002/zamm.19870670315.
- [12] R. Sankarasubramanian and W. N. Gill, Taylor diffusion in laminar flow in an eccentric annulus, *International Journal of Heat and Mass Transfer* **14**(7) (1971), 905 – 919, DOI: 10.1016/0017-9310(71)90117-7.
- [13] R. Sankarasubramanian and W. N. Gill, Unsteady convective diffusion with interphase mass transfer, *Proceedings of the Royal Society of London A: Mathematical, Physical and Engineering Sciences* **333**(1592) (1973), 115 – 132, DOI: 10.1098/rspa.1973.0051.

- [14] A. Sarkar and G. Jayaraman, Nonlinear analysis of oscillatory flow in the annulus of an elastic tube: Application to catheterized artery, *Physics of Fluids* **13** (2001), 2901 – 2912, DOI: 10.1063/1.1389285.
- [15] A. Sarkar and G. Jayaraman, The effect of wall absorption on dispersion in annular flows, *Acta Mechanica* **158** (2002), 105 – 119, DOI: 10.1007/BF01463173.
- [16] G. I. Taylor, Dispersion of soluble matter in solvent flowing slowly through a tube, *Proceedings of the Royal Society of London A: Mathematical, Physical and Engineering Sciences* **219**(1137) (1953), 186 – 203, DOI: 10.1098/rspa.1953.0139.
- [17] A. Tiwari and S. Deo, Pulsatile flow in a cylindrical tube with porous walls: applications to blood flow, *Journal Porous Media* **16**(4) (2013), 335 – 340, DOI: 10.1615/JPorMedia.v16.i4.50.
- [18] B. Umadevi, P. A. Dinesh, R. R. Indira and C. V. Deo, The effect of particle drag and wall absorption on mass transfer in concentric annulus flows, *Mapana Journal of Sciences* **10**(1) (2011), 1 – 13, DOI: 10.12723/mjs.18.1.
- [19] K. V. Venkataswamy, S. Jagadeesha and R. Indira, An analytical study of dispersion and wall absorption with effect of viscoelasticity and magnetic field, *Journal of Informatics and Mathematical Sciences* **11**(3-4) (2019), 433 – 439, DOI: 10.26713/jims.v11i3-4.1347.

